Journal of Materials Chemistry A

COMMUNICATION

View Article Online
View Journal | View Issue

Cite this: J. Mater. Chem. A, 2019, 7, 1996

Received 11th November 2018
Accepted 3rd January 2019

DOI: 10.1039/c8ta10847a

rsc.li/materials-a

Photo-to-electricity generation of aligned carbon nanotubes in water†

Yajie Hu,‡[a] Sisi He,‡[a] Xiaojie Xu,[a] Longsheng Zhang,[a] Yifan Xu,[a] Jing Zhang,[a] Peng Liu,[a] Yunzhou Wen,[a] Fenglou Ni,[a] Mengwen Jia,[b] Bo Zhang,[a] Xuemei Sun,[a] Peining Chen*[a] and Huisheng Peng*[a]

The photovoltaic effect occurs at the interface between two different types of semiconductors that are joined together to create a p–n junction, and it has been explored as a basic principle to harvest solar energy to generate electricity. The active materials are typically protected from water for stable performances, and the photovoltaic effect is observed in photovoltaic materials with appropriate energy bands and interfaces. Here we have discovered another new and general photo-to-electricity phenomenon in semiconducting materials in water. The photo-to-electricity conversion could be realized by using the identical type of semiconductor as the active material. Aligned carbon nanotube sheets were demonstrated to output high open-circuit voltages up to 0.48 V. Due to the intrinsic flexibility of the designed carbon nanotube sheets, the output voltage could be well maintained after deforming for 8000 cycles.

Mankind has utilized solar energy by converting sunlight to electricity for more than one hundred years since the photovoltaic effect was first observed in 1839.[1–6] The photovoltaic effect generally occurs at the interface between two different types of semiconductors that are joined together to create a p–n junction.[7,8] Photovoltage is generated as the distribution of charge carriers in the region of the p–n junction changes upon exposure to sunlight with sufficient energy. The photovoltaic effect has been observed at the p–n junction formed in semiconducting materials including silicon,[9,10] conjugated polymers[11,12] and perovskites,[13,14] and several kinds of photovoltaic cells based on the photovoltaic effect have been developed for the utilization of solar energy.[15–17] Generally, the active materials should be carefully sealed to protect them from water for stable performances.[18,19] In addition, the typical photovoltaic effect requires a careful selection of active materials with appropriate energy bands and interfaces with limited sources.[20–22]

Herein, we report a new and general photo-to-electricity phenomenon using identical semiconductors as the active material in water. Carbon nanotubes (CNTs) were assembled into an aligned CNT sheet as the semiconducting active material to demonstrate this unexpected discovery. Due to the combined excellent electronic and mechanical properties, the aligned CNT sheet also simultaneously served as the electrode for the above photo-to-electricity conversion. The semiconducting property of the aligned CNT sheet and the electron transfer from OH· radicals to OH^- anions at the interface between water and the CNT sheet were found to play a critical role in electricity generation. A high open-circuit voltage of 0.48 V was produced from the new photo-to-electricity phenomenon. Due to the intrinsic flexibility of the designed CNT sheet, the output voltage could be well maintained after deformation for 8000 cycles.

We assembled two identical aligned CNT sheets with a separator between them (Fig. 1a). The separator was used to keep these two electrodes physically apart from each other to avoid short circuit. The spinnable CNT array was synthesized by using the chemical vapor deposition method (Fig. S1†).[23–25] The CNT sheet could be continuously drawn from the CNT array due to the existence of relatively strong adjacent van der Waals interactions between the neighboring CNT bundles.[26] The obtained CNT sheet consisting of tens of thousands of CNTs with a high degree of alignment was freestanding and flexible (Fig. 1b). As shown in Fig. 1c, the CNTs exhibited a typical multi-walled structure with an average diameter of ~8 nm. Due to the intrinsic flexibility of the aligned CNT sheet, the resulting system was flexible and could be bent and even curled (Fig. 1d). The voltage between the two CNT sheets was monitored to characterize the system performance. It was found that there was no voltage generated when the system was put into pure water with no light irradiation on the device. Interestingly, we

[a]State Key Laboratory of Molecular Engineering of Polymers, Department of Macromolecular Science and Laboratory of Advanced Materials, Fudan University, Shanghai 200438, China. E-mail: peiningc@fudan.edu.cn; penghs@fudan.edu.cn

[b]State Key Laboratory of Surface Physics, Department of Physics and Laboratory of Advanced Materials, Fudan University, Shanghai 200438, China

† Electronic supplementary information (ESI) available. See DOI: 10.1039/c8ta10847a

‡ These authors contributed equally to this work.

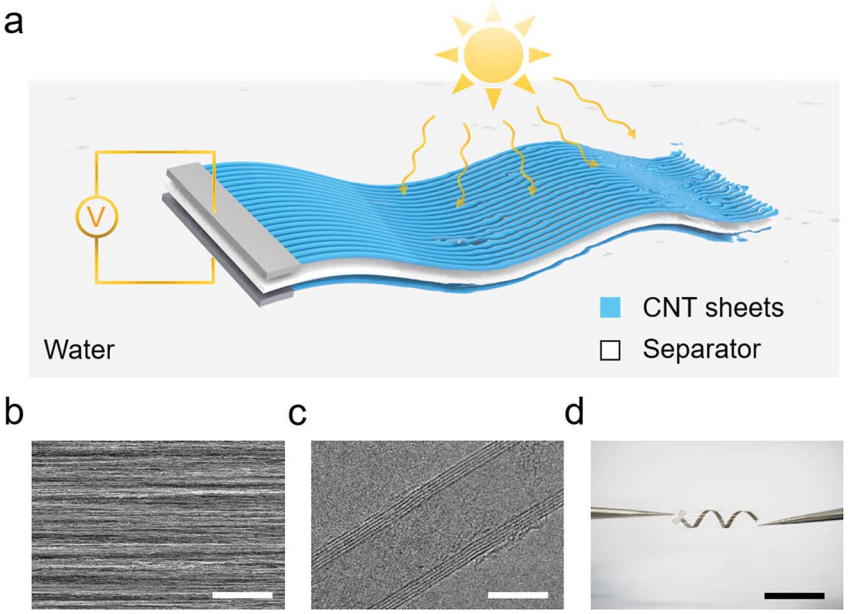

Fig. 1 (a) Schematic illustration of the experimental setup for measuring electricity generation from the new photo-to-electricity system. (b) Scanning electron microscopy image of the CNT sheet. (c) Transmission electron microscopy image of the CNT. (d) Photograph of a photo-to-electricity system under curling. Scale bars: 50 μm, 5 nm and 1 cm in (b, c and d), respectively.

observed an open-circuit voltage of 0.17 V when the upper CNT sheet was exposed to simulated solar irradiation while there was no obvious voltage generated when both sides were exposed to light (Fig. 2a). In addition, the open-circuit voltage was well maintained with irradiation for 1000 s, showing the high stability of the new photo-to-electricity system (Fig. S2†). Meanwhile, a short-circuit current was also detected when a circuit was formed (Fig. S3†). A similar photo-to-electricity phenomenon was also observed when the system was fabricated in a fiber format (Fig. S4†). Due to the intrinsic flexibility

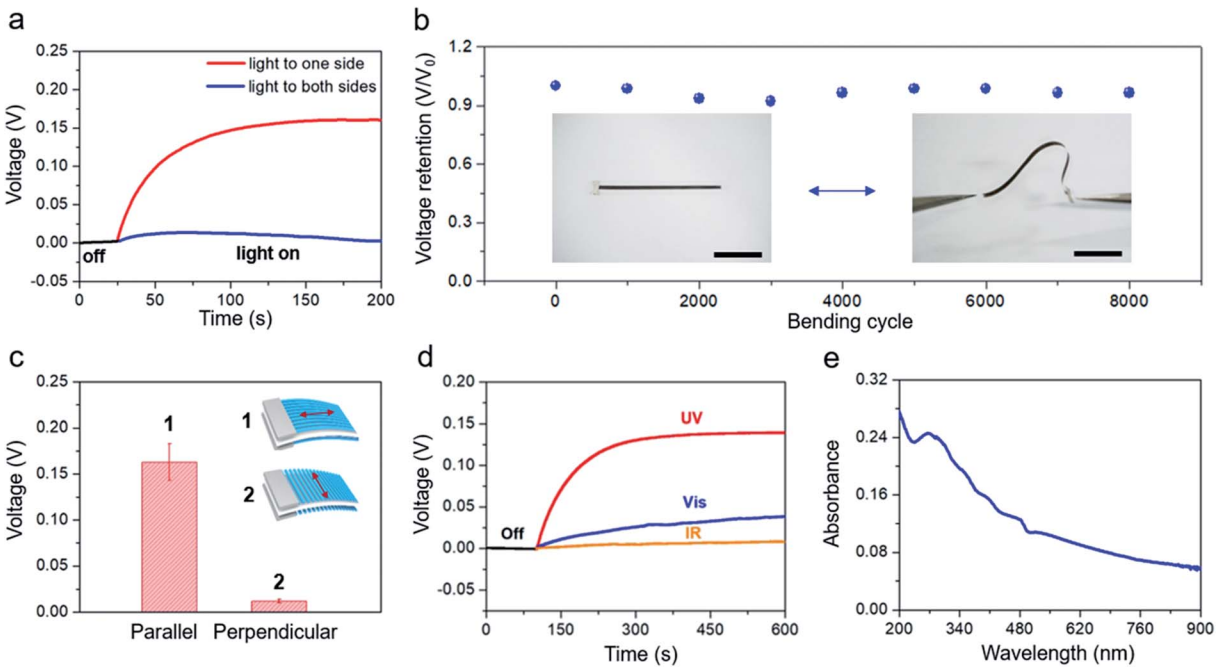

Fig. 2 Photo-to-electricity conversion under light irradiation in deionized water. (a) Open-circuit voltage upon light irradiation. (b) The voltage output after deformation for 8000 cycles (inset: photographs of the photo-to-electricity system in a flat state and under bending. Scale bar: 1 cm). (c) Dependence of the open-circuit voltage on the alignment direction of the CNT sheets (inset: schematic illustration of the parallel and perpendicular alignment of the CNTs in the sheet). (d) Dependence of the open-circuit voltage on the wavelength of light. (e) UV-Vis absorption spectrum of the CNT sheet. The size of the CNT sheet (a–e) was 1 mm × 2.5 cm, and the light intensity was 150 mW cm^{-2}.

of the CNT sheets, the voltage output was stable and no obvious degradation occurred after 8000 cycles of deformations (Fig. 2b).

The photo-to-electricity generation was greatly influenced by the alignment direction of the CNTs. A voltage of 0.17 V was achieved when the alignment of CNTs was designed to be parallel to the length direction of the CNT sheet (inset in Fig. 2c). However, the voltage drastically decreased to 0.012 V when the CNTs were perpendicular to the length direction of the CNT sheet (Fig. 2c). This great distinction might be derived from the different electrical properties of CNT sheets with different alignment directions, *i.e.*, the resistance of the former was much lower than that of the latter, indicating that the electrons were much easier to transfer along the CNTs when they had been aligned along the length direction of the sheet (Fig. S5†). For the convenience of discussion, the photo-to-electricity system with the CNTs being parallel to the length direction of the CNT sheet was studied unless specified otherwise.

The photo-to-electricity generation in water also varied with the applied illumination at different wavelengths. For instance, we found that no obvious voltage output was detected when the system was exposed to infrared light. However, a voltage of 0.04 V was generated when visible light (420–780 nm) was applied, and a higher voltage of 0.14 V was observed under ultraviolet light with wavelengths from 200 to 400 nm (Fig. 2d). The generated current was also studied and similar trends were observed (Fig. S6†). This difference might be attributed to the characteristic absorption of CNT sheets. To confirm this, we measured the absorption spectrum of CNT sheets. It revealed that CNT sheets mainly absorbed ultraviolet light as the absorption spectrum showed an absorption peak at 234 nm (Fig. 2e). In addition, in consideration of the broad peak, the CNT sheets might also absorb a small amount of visible light, but barely any infrared light was absorbed. The light absorption selectivity of the CNT sheets was well consistent with the varied voltage output of the system upon light illumination at different wavelengths.

Based on the photo-to-electricity experimental results, a working mechanism is proposed in Fig. 3a and b. As a preliminary to systematic mechanism analysis, the semiconductor property of the aligned CNT sheets was first investigated. Here, we traced the electrical resistances of the CNT sheets with increasing temperature (Fig. S7†). The resistances of the aligned CNT sheets decreased with the increase of temperature. The resistivity–temperature curve revealed that the aligned CNT sheets showed a semiconductor characteristic as the curve had a negative slope of dR/dT.[27,28] The semiconductor characteristics of the CNT sheet could be explained by the previously reported three-dimensional-hopping mechanism,[29,30] where the electrons are inclined to hop from one CNT (or CNT bundle) to the neighboring ones. We also carried out the measurement of Hall resistance to further confirm the semiconductor property of the aligned CNT sheets (Fig. S8†). As the Hall coefficient $R_H = tR_{xy}/B$, where R_{xy} is the Hall resistance, t is the sample thickness, and B is the magnetic field intensity, an obvious negative value of the Hall coefficient was observed due to the negative slope of the Hall resistance–magnetic field curve. Hence, the CNT sheets exhibited a typical n-type semiconductor behavior and the carriers of the CNT sheets were mainly electrons,[31] which may play an important role in the photo-to-electricity generation in water.

When there was no light irradiation or the same light irradiation on both sides, the Fermi levels of the two CNT sheets were at the same position and there was no voltage generation (Fig. 3a). However, when the photo-to-electricity system was exposed to asymmetric light irradiation, a difference in the Fermi level position of the two electrodes was resulted and voltage could be generated. More specifically, as one side of the CNT sheets was exposed to light, photons with sufficient energy exceeding that of the CNT sheet bandgap were absorbed due to the semiconducting property of the aligned CNT sheets (Fig. 3b). Then, the photo-induced electrons migrated to the conduction band of the CNT sheets, while holes moved to the valence band, leading to an upward shift of the Fermi level. As the Fermi level of the CNT sheets was higher than the redox potential of deionized water, electrons would flow from the CNT sheets to the water until an electrical equilibrium was reached. An electrical potential difference across the solid–liquid interface was generated, which worked in Schottky barrier mode. The accumulation of positive charges was resulted and a space charge region was produced on each side of the semiconductor–liquid heterojunction.[32] Hence, internal built-in potential was observed and served as the driving force to separate the photo-generated electron–hole pairs. As a result, the separated holes moved from the valence band of the CNT sheets to the CNT/water interface and got captured by the OH^- anions to form $OH\cdot$ radicals ($h^+ + OH^- \rightarrow OH\cdot$).[33] Meanwhile, the separated electrons moved from the conduction band of the irradiated CNT sheets into the external circuit and reached the counter electrode composed of CNT sheets which had not been irradiated by light. Finally, the electrons returned to the OH− radicals to form OH^- anions and the voltage and current were thus generated.

To further verify our mechanism, electron paramagnetic resonance (EPR) was used to detect the $OH\cdot$ radicals during the photo-to-electricity generation process (Fig. 3c). No obvious EPR signal was observed when there was no light irradiation. Upon exposure to light, the characteristic peaks of 5,5-dimethyl-1-pyrroline-*N*-oxide (DMPO)-$OH\cdot$ with an intensity ratio of 1 : 2 : 2 : 1 were detected, indicating the generation of $OH\cdot$ radicals.[34,35] To avoid the influence of water itself on exposure to light, we also tested the EPR signal of water when exposed to light, and no obvious characteristic peaks of DMPO-$OH\cdot$ were detected. These results further confirmed that the electrons transferred from the $OH\cdot$ radicals to form OH^- anions in water and a circuit was formed. We further observed that the EPR signals of DMPO-$OH\cdot$ increased with the increase of light intensity (Fig. 3d and S9†). A similar trend was also found in the dependence of current density on light intensity (Fig. 3e). In other words, irradiation light with higher intensity contributes to the production of more $OH\cdot$ to enhance the electricity output, which is well consistent with the proposed mechanism. Moreover, it was found that electricity generation could also be observed when the system was put in other polar solvents such

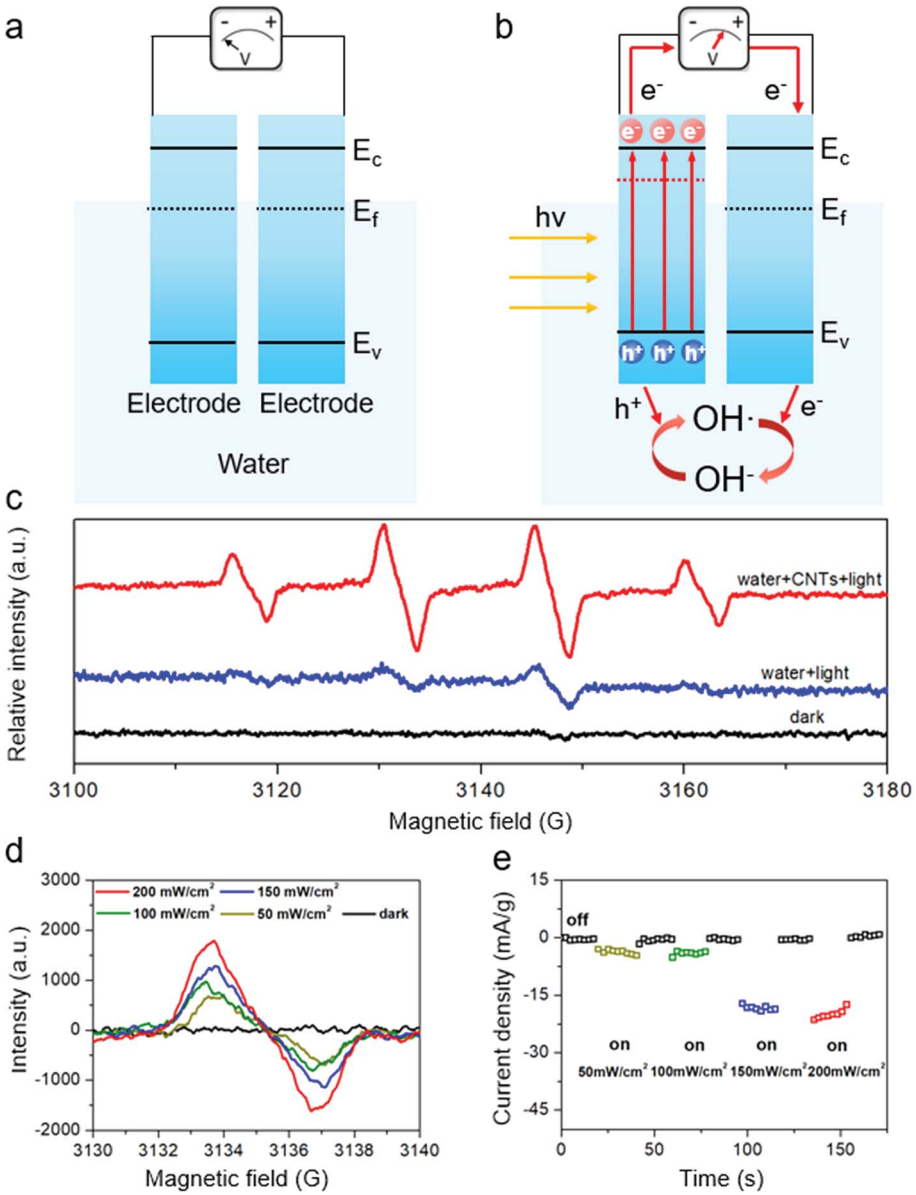

Fig. 3 Mechanism of the photo-to-electricity conversion. (a) and (b) Energy level diagrams of the photo-to-electricity system without light irradiation and under light irradiation, respectively. The red line indicates the flow direction of the electrons. (c) EPR signals of DMPO-OH· (aqueous solution) for the electricity generation process. (d) Locally enlarged EPR signals of DMPO-OH· (aqueous solution) when the device was exposed to light with different intensities. (e) Dependence of the current densities on light intensities.

as ethanol, ethylene glycol, DMF and DMSO due to the existence of polar groups (Fig. S10 and S11†). Therefore, it is easy to understand that there was no electricity generation in nonpolar solvents without polar groups (Fig. S12 and S13†). According to the proposed mechanism, the generated current can be enhanced by increasing the concentration of OH^-, which was consistent with the experimental results that the generated current in alkaline solution was higher than that in acidic and neutral solutions (Fig. S18†). Inspired by this mechanism, the photo-to-electricity generation could also be observed among other kinds of organic and inorganic semiconducting materials in water such as poly(3-hexyl thiophene) and ZnO (Fig. S19 and S20†), and stable voltage outputs of 0.2 and 0.09 V were, respectively, generated upon sunlight irradiation.

The new photo-to-electricity system can be readily fabricated on a large scale with high flexibility (Fig. 4a). In this way, the current could be greatly enhanced with the increasing absorption area. Besides, the voltage can be efficiently improved by using composite electrodes. Composite electrodes were prepared by integrating another well studied semiconductor, ZnO, into the CNT sheets through a dip-coating process. A higher output with a voltage of 0.48 V was achieved (Fig. 4b) compared with the voltage produced by the photo-to-electricity systems based on CNTs or ZnO (Fig. 4c). Besides the additional contribution of ZnO to the electricity output upon light irradiation due to the semiconductor property, the enhancement in the voltage output for the composite electrode might also be attributed to the synergy effect of CNTs and ZnO, that is, the

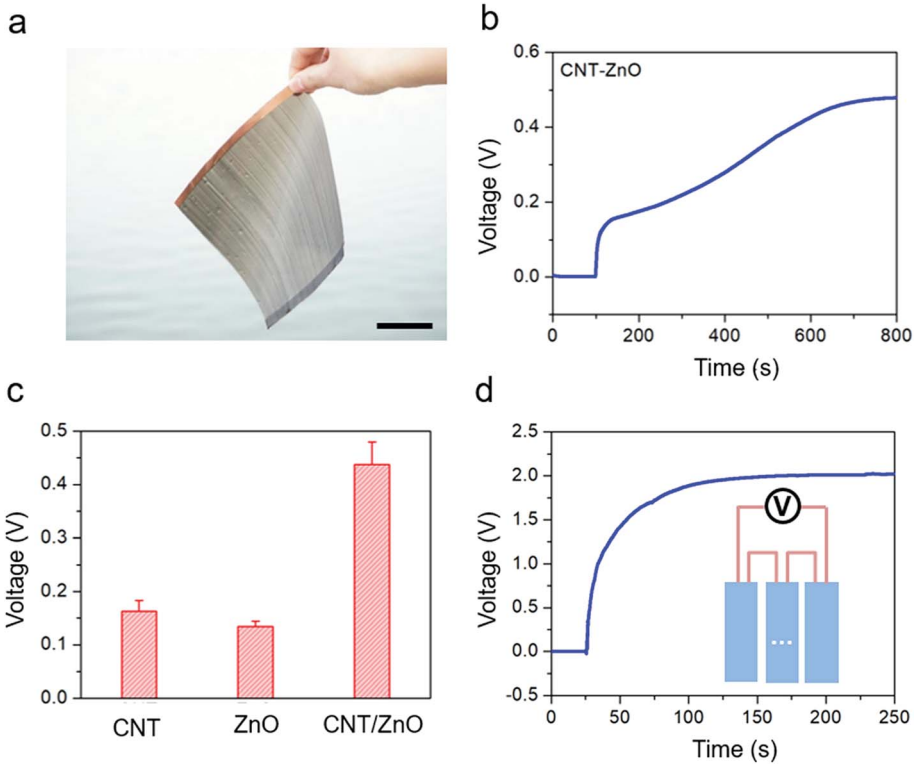

Fig. 4 Enhanced electricity outputs of the photo-to-electricity systems. (a) Photograph of the light-to-electricity system with large size. The size of the photo-to-electricity system was 15 cm × 15 cm. Scale bar: 5 cm. (b) Open-circuit voltage of the photo-to-electricity system based on the aligned CNT/ZnO composite film. (c) Comparison of the open-circuit voltages based on the as-synthesized CNT sheet, ZnO and aligned CNT/ZnO composite film. (d) Open-circuit voltage of the photo-to-electricity system based on the aligned CNT/ZnO composite film in series (inset: circuit diagram). The size of the CNT sheet (b–d) was 1 mm × 2.5 cm, and the light intensity was 150 mW cm^{-2}.

interaction between ZnO and CNTs could efficiently enhance the electron transfer and reduce the electron–hole pair recombination.[36] The output voltages and currents could be greatly improved by connecting several photo-to-electricity systems in series and in parallel, respectively. For instance, when ten systems were connected in series, the light-induced voltage could be increased to 2 V (Fig. 4d) to light up a red light-emitting device (Fig. S21†). In addition, the electricity output could be further enhanced through the optimization of semiconducting materials as well as the optimal structural design of the photo-to-electricity system. This new photo-to-electricity phenomenon may provide a new and effective approach to power electronic devices such as underwater sensors, micro-vehicles and robotics in water environments.

In summary, a new photo-to-electricity phenomenon was observed for semiconducting materials in water. When the aligned CNT sheet was used as the active and electrode materials, a high output voltage of 0.47 V was achieved. The photo-induced electrons or holes from the CNT sheets, involved in the reversible conversion between OH· radicals and OH^- anions at the water/CNT interface, play a critical role in the electricity generation. The proposed mechanism could also be generalized to the other organic and inorganic semiconducting materials. This new photo-to-electricity conversion may provide a general and effective approach to meet the energy requirements for electronic devices in water environments.

Author contributions

Y. J. H. and S. S. H. contributed equally to this work. H. S. P. and P. N. C. provided research direction and supervised the project. Y. J. H. and S. S. H. designed the research. Y. J. H., S. S. H., X. J. X., L. S. Z. and M. W. J. carried out the experiments and analyzed the data. Y. F. X., P. L., Y. Z. W., F. L. N., J. Z., B. Z. and X. M. S. contributed to analyzing the data and discussion. J. Z. drew the schematic illustration. Y. J. H., S. S. H., X. J. X. and P. N. C. wrote the paper. All authors reviewed and revised the manuscript.

Conflicts of interest

There are no conflicts to declare.

Acknowledgements

This work was supported by the MOST (2016YFA0203302), NSFC (21634003, 51573027, 51673043, 21604012, 21805044, and 21875042), STCSM (16JC1400702, 17QA1400400, 18QA1400700, and 18QA1400800), SHMEC (2017-01-07-00-07-E00062) and Yanchang Petroleum Group.

References

1 H. Heywood, *Nature*, 1957, **180**, 115–118.

2 S. Chu and A. Majumdar, *Nature*, 2012, **488**, 294–303.
3 S. Chu, Y. Cui and N. Liu, *Nat. Mater.*, 2016, **16**, 16–22.
4 M. A. Green and S. P. Bremner, *Nat. Mater.*, 2017, **16**, 23–34.
5 Y. Cai, L. Huo and Y. Sun, *Adv. Mater.*, 2017, **29**, 1605437.
6 C. T. Howells, S. Saylan, H. Kim, K. Marbou, T. Aoyama, A. Nakao, M. Uchiyam, I. D. W. Samuel, D.-W. Kim, M. S. Dahlem and P. Andre, *J. Mater. Chem. A*, 2018, **6**, 16012–16028.
7 C.-H. Chiang and C.-G. Wu, *Nat. Photonics*, 2016, **10**, 196–200.
8 Y. Yang, W. Chen, L. Dou, W.-H. Chang, H.-S. Duan, B. Bob, G. Li and Y. Yang, *Nat. Photonics*, 2015, **9**, 190–198.
9 S. Jeong, M. D. McGehee and Y. Cui, *Nat. Commun.*, 2013, **4**, 2950.
10 F. Priolo, T. Gregorkiewicz, M. Galli and T. F. Krauss, *Nat. Nanotechnol.*, 2014, **9**, 19–32.
11 H. Bin, L. Gao, Z.-G. Zhang, Y. Yang, Y. Zhang, C. Zhang, S. Chen, L. Xue, C. Yang, M. Xiao and Y. Li, *Nat. Commun.*, 2016, **7**, 13651.
12 J.-Q. Wang, S.-K. Xie, D.-Y. Zhang, R. Wang, Z. Zheng, H.-Q. Zhou and Y. Zhang, *J. Mater. Chem. A*, 2018, **6**, 19934–19940.
13 J. Jeong, H.-B. Kim, Y. J. Yoon, N. G. An, S. Song, J. W. Kim, M. Kim, H. Jang, D. S. Kim, G.-H. Kim and J. Y. Kim, *J. Mater. Chem. A*, 2018, **6**, 20138–20144.
14 W. S. Yang, J. H. Noh, N. J. Jeon, Y. C. Kim, S. Ryu, J. Seo and S. Seok, *Science*, 2015, **348**, 1234–1237.
15 Z. Li, K. Jiang, G. Yang, J. K. L. Lai, T. Ma, J. Zhao, W. Ma and H. Yan, *Nat. Commun.*, 2016, **7**, 13094.
16 H. Yao, L. Ye, J. Hou, B. Jang, G. Han, Y. Cui, G. M. Su, C. Wang, B. Gao, R. Yu, H. Zhang, Y. Yi, H. Y. Woo, H. Ade and J. Hou, *Adv. Mater.*, 2017, **29**, 1700254.
17 S. Venkatesan, I.-P. Liu, J.-C. Lin, M.-H. Tsai, H. Teng and Y.-L. Lee, *J. Mater. Chem. A*, 2018, **6**, 10085–10094.
18 Y. Han, S. Meyer, Y. Dkhissi, K. Weber, J. M. Pringle, U. Bach, L. Spiccia and Y.-B. Cheng, *J. Mater. Chem. A*, 2015, **3**, 8139–8147.
19 M. I. Asghar, J. Zhang, H. Wang and P. D. Lund, *Renewable Sustainable Energy Rev.*, 2017, **77**, 131–146.
20 S. Chen, Y. Liu, L. Zhang, P. C. Y. Chow, Z. Wang, G. Zhang, W. Ma and H. Yan, *J. Am. Chem. Soc.*, 2017, **139**, 6298–6301.
21 H. Zhou, L. Yang, S. C. Price, K. J. Knight and W. You, *Angew. Chem., Int. Ed.*, 2010, **122**, 8164–8167.
22 H. Yao, Y. Cui, R. Yu, B. Gao, H. Zhang and J. Hou, *Angew. Chem., Int. Ed.*, 2017, **56**, 3045–3049.
23 P. Chen, Y. Xu, S. He, X. Sun, S. Pan, J. Deng, D. Chen and H. Peng, *Nat. Nanotechnol.*, 2015, **10**, 1077–1083.
24 J. Ren, Y. Zhang, W. Bai, X. Chen, Z. Zhang, X. Fang, W. Weng, Y. Wang and H. Peng, *Angew. Chem., Int. Ed.*, 2014, **53**, 7864–7869.
25 Y. Zhang, W. Bai, X. Cheng, J. Ren, W. Weng, P. Chen, X. Fang, Z. Zhang and H. Peng, *Angew. Chem., Int. Ed.*, 2014, **53**, 14564–14568.
26 A. A. Kuznetsov, A. F. Fonseca, R. H. Baughman and A. A. Zakhidov, *ACS Nano*, 2011, **5**, 985–993.
27 H. Peng, *J. Am. Chem. Soc.*, 2008, **130**, 42–43.
28 T. Matsuoka and K. Shimizu, *Nature*, 2009, **458**, 186–189.
29 Q. Li, Y. Li, X. Zhang, S. B. Chikkannanavar, Y. Zhao, A. M. Dangelewicz, L. Zheng, S. K. Doorn, Q. Jia, D. E. Peterson, P. N. Arendt and Y. Zhu, *Adv. Mater.*, 2007, **19**, 3358–3363.
30 H. Peng, X. Sun, F. Cai, X. Chen, Y. Zhu, G. Liao, D. Chen, Q. Li, Y. Lu, Y. Zhu and Q. Jia, *Nat. Nanotechnol.*, 2009, **4**, 738–741.
31 D. LeBoeuf, N. Doiron-Leyraud, J. Levallois, R. Daou, J. Bonnemaison, N. Hussey, L. Balicas, B. Ramshaw, R. Liang, D. Bonn, W. Hardy, S. Adachi, C. Proust and L. Taillefer, *Nature*, 2007, **450**, 533–536.
32 M. Gratzel, *Nature*, 2001, **414**, 338–344.
33 W. Lee and M. Hon, *Appl. Phys. Lett.*, 2011, **99**, 251102.
34 C. Su, X. Duan, J. Miao, Y. Zhong, W. Zhou, S. Wang and Z. Shao, *ACS Catal.*, 2017, **7**, 388–397.
35 R. Li, Y. Weng, X. Zhou, X. Wang, Y. Mi, R. Chong, H. Han and C. Li, *Energy Environ. Sci.*, 2015, **8**, 2377–2382.
36 G. Zhu, H. Wang, G. Yang, L. Chen, P. Guo and L. Zhang, *RSC Adv.*, 2015, **5**, 72476–72481.